

DESIGN, FABRICATION AND OPERATION OF A DEVICE FOR MANUFACTURING METAL FOAMS AND COMPOSITES BY INFILTRATION

J. C. Carranza , B. Y. Casas  and I. Alfonso 

Instituto de Investigaciones en Materiales, Unidad Morelia, Universidad Nacional Autónoma de México, Campus Morelia UNAM, Antigua Carretera a Pátzcuaro No. 8701, Col. Ex-Hacienda de San José de la Huerta, C.P. 58190 Morelia, Michoacán, Mexico

I. A. Figueroa 

Instituto de Investigaciones en Materiales, Universidad Nacional Autónoma de México, Circuito Exterior S/N, Cd. Universitaria, C.P. 04510 Mexico city, Mexico

L. E. Carranza 

Facultad de Ingeniería Mecánica, Universidad Michoacana de San Nicolás de Hidalgo, Edificio W, Ciudad Universitaria, CP 58000 Morelia, Michoacán, Mexico

Copyright © 2023 The Author(s)
<https://doi.org/10.1007/s40962-023-00979-x>

Abstract

This work presents the design and fabrication of a simple device for manufacturing metal foams and composites using infiltration. The particularities of the operation of this device are also included here, detailing examples of materials manufactured using it. This device was thought to produce composites and foams using matrices from low to medium melting points (e.g., from Mg to Cu alloys), limited to ~ 1200 °C. It can be used to produce samples large enough for their study and characterization, being cheaper than other devices reported in literature. Foams and composites of different sizes can be manufactured depending on the dimensions of the device, which can be modified according to the necessities. As examples, cylindrical (10 cm height and 5 cm in diameter) samples were manufactured infiltrating Al and Cu alloys on NaCl, NaCl- Al_2O_3 spheres mixture, and iron hollow spheres, for

manufacturing respectively conventional, composite and syntactic foams. These materials were analyzed through Optical and Scanning Electron Microscopies (OM and SEM, respectively), and compression tests. Their densities and porosities were also measured. The analysis of the obtained materials revealed that following the correct experimental conditions, composites and foams without defects can be manufactured using this device. Different porosity and reinforcement percentages were obtained under these conditions, with the expected mechanical behaviors of such materials.

Keywords: foams, composites, device, infiltration, space holder

Introduction

Metal foams have proven to be materials with a wide range of mechanical properties and applications. These properties include good heat transfer, vibration and sound absorption, permeability, compression resistance, and biocompatibility. Their combinations make metal foams

suitable materials for applications which, in some cases, can even replace the solid materials traditionally used. These properties and applications have been reviewed, as shows the research of Baumgartner and Gers,¹ who discussed how some automotive components can get higher stiffness using foam cores instead of solid alloys, reducing weight for the car body. In the reviews of Banhart,² and Gibson and Ashby,³ authors presented in detail the characteristics, properties and applications of cellular solids in general, and metallic foams in particular. The use of

reinforcements to obtain composite and syntactic foams has also increased in the last years, as shows the work of Rabiei and Vendra⁴ comparing different metal foams, or the works of Binesh et al.⁵ and Bolat et al.⁶ Composite metal foams are porous metal matrices commonly reinforced with solid ceramics, such as Carbon nanotubes, SiC, TiC, TiO₂, Al₂O₃, MgO and BN,⁷ depending their mechanical properties mainly on the relative quantities of porosity and reinforcement, and on the characteristics of the reinforcement, which can be nanotubes,⁸ fibers,⁹ particles,¹⁰ and whiskers, among other shapes.⁷ On the other hand, syntactic foams (a special case of composite foams) have the particularity of being metal matrices reinforced with hollow materials, such as hollow Fe spheres (works of Rabiei and Vendra,⁴ or Szlancsik et al.¹¹), or hollow spheres made of the above commented ceramic reinforcements.⁷ New works have also included reinforcements such as expanded glass,⁶ pumice,¹² fly ash¹³ and expanded clay.¹⁴ An example of a hybrid composite-foam material is presented in the work of Károlyi et al.¹⁴ who studied graded aluminum matrix syntactic foams combining as reinforcements expanded clay aggregates and Al₂O₃ hollow spheres. These authors demonstrated that the effective properties of the metal foams can fulfill industrial requirements by simply varying the distribution of the filler materials.

Aluminum and its alloys are the most reported matrices for both conventional and composite foams,¹²⁻¹⁵ although Cu, Ti, Mg and their alloys have been also reported, as show recognized works about these materials by Banhart^{2,16} and by Gibson and Ashby.³ Composite foams have higher mechanical properties than conventional foams due to their reinforcements, but remaining a low density. If a composite foam is free of porosity, it becomes in a composite material, with higher mechanical properties, but also with a higher density, as established the works of Ajay et al.¹⁷ and Sentil et. al.¹⁸ These four types of materials (conventional foams, composite foams, syntactic foams and composites) have countless and varied applications. Conventional foams are used as impact absorbers, noise reduction systems, dust and fluid filters, heat exchangers, catalysis supporters, flame arresters, as structural material, or as parts of lightweight panels in automotive, aeronautical or naval industries.^{2,3} The works of Rabiei and Vendra,⁴ and Bolat et al.¹⁹ report that syntactic foams are useful in marine equipment, sandwich parts in composite materials, and structural components in automotive, construction and aerospace industries. On the other hand, composite or hybrid foams have applications which include transportation, aerospace and military industries, tools, and human health care.^{8,14} They can replace some solid materials while reducing weight and retaining material properties. Finally, composite materials have been the most studied among these four kind of materials, and their applications depend among other parameters on the kind, size and distribution of the reinforcement. This leads to a wide variety of physical and mechanical properties, with

applications in industries such as transport, aeronautic, aerospace and electric, besides in a wide variety of recreational products and sporting goods.^{7-10,17,18} These four materials can be manufactured using similar processes, because they have in common a metal matrix and a second phase, which can be solid, porous, or their combinations.

According to Banhart,¹⁶ there are two basic ways for manufacturing metallic foams: (i) direct foaming methods, starting from a molten metal, and (ii) indirect foaming methods, in which the process begins from a solid precursor. Replication is among these methods, which were first studied by Polonsky et al.,²⁰ who found that it is possible to obtain interconnected open cell foams by infiltrating in a first step a solid preform or a “foam negative” with molten metal, and then in a second step eliminating the preform by shaking, burning or dissolving the material with a suitable solvent. When powder metallurgy (PM) is applied, this technique is called space-holder leaching, as established Baumgartner and Gers.¹ NaCl,^{21,22} naphthalene,²³ saccharose²⁴ and potassium bromide²⁵ are among the most used space holders.²⁶ New techniques such as microwave sintering has provided to be excellent routes to obtain new foams, as shows the work of Akinwekomi et al.¹³ for manufacturing aluminum-fly ash syntactic foams. The use of an industrial-focused die casting machine has demonstrated the possibility of manufacturing hybrid aluminum matrix syntactic foams reinforced with pumice and expanded glass not only at lab scales.²⁷ Another example of new manufacturing processes to obtain advanced foams is the work of Bolat et al.²⁸ who produced Al-7075 matrix foams reinforced with 2-4 mm pumice particles by sandwich infiltration casting. In the manufacturing processes of composites and syntactic foams through infiltration, molten metal flows on the reinforcements or hollow materials, being obtained the final material without the necessity of the second step (preform removal) to generate the porosity. Due to the use of these preforms, reinforcements, or space holder phases, through their replication it is possible to highly control the material topology, as it is the case of the pores or reinforcements percentages, distribution and size. The use of infiltration as a replication casting process allows to obtain foams or composites with better mechanical properties, compared to materials obtained by PM. This because pore walls are solid. Besides, using optima infiltration variables, it is possible to fill all the spaces between the space holders or reinforcements. In this process, there are 3 key factors: (1) the pressure needed to promote infiltration, (2) the melting temperature of the metal or alloy to be melted for infiltrating the preform, and (3) the characteristics of the preform to be used (particle size, material, previously sintered or not preform, etc.).²⁹ It has been found that the control of these parameters allows a wide variety of possibilities of manufacturing, with distinct characteristics. For example, the use of uniformly sized NaCl or fractal distributions as space holders results in foams with different porosities and

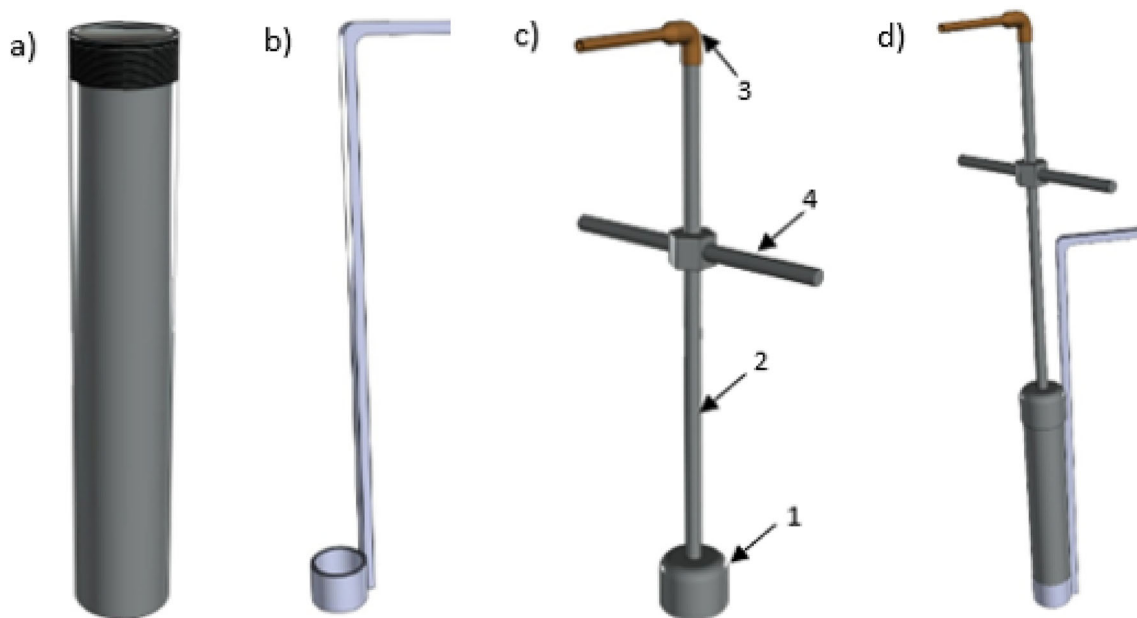


Figure 1. Main components of the infiltration device: (a) Infiltration chamber, (b) Spoon, (c) Cover, and (d) Complete layout.

properties, as we studied in a previous work manufacturing foams by the infiltration method.²¹

The infiltration process is very simple, as it is described in the work of Lara-Rodriguez et al.²² Metal foams and composites can be manufactured by this method using gas pressure to ensure infiltration without defects (avoiding cell rupture, melt drainage, etc.), ensuring the required physical and mechanical properties.^{22,30} Nevertheless, the devices used to produce these materials sometimes are too complex or have expensive components, as Banhart² commented in his review about foam properties and manufacturing processes. An example is the work of Lara-Rodriguez et al.,²² who designed a device for this purpose. Then, it is necessary to improve the manufacturing process and try to find a simpler and cheaper device, without losing the efficacy of the infiltration process. According to this, we are proposing a new low-cost device for manufacturing foams and composites by infiltration. The present work includes the design, manufacturing, and operation of this device, which has advantages compared to other devices reported in literature. Different conventional, composite and syntactic foams were experimentally manufactured using this device, infiltrating different space holder and reinforcement particles. Such obtained materials were characterized in order to probe the effectiveness of the device.

Design and Experimental Parts

Design of the Device

The design of the device presented in this work was made trying to include advantages, such as easy manufacturing

and assembly, low cost, and a cheaper manufacturing process. An in deep literature search allowed us to define these points and try to improve each detail that could affect the process. Figure 1a–d shows the complete device resulting from this analysis, drawn using SOLIDWORKS Premium 2022 SP2.0. It contains three main components: (i) the infiltration chamber, in which the infiltration process occurs (Figure 1a); (ii) a tool called “spoon” due to its shape (see Figure 1b), for the device holding and manipulation; and (iii) a cover (Figure 1c), composed by the cover itself (1), and by a conduction tube (2), a nozzle (3) where gas can be injected, and a bar (4) for handling the device. The infiltration chamber is a simple pipe open on both sides, with its top threaded to be sealed with the cover. Different joints are used in our design, as can be seen in Fig. 1c, where the cover (1) and handle (4) are welded to the conduction tube (2). This tube is threaded at the top to connect to the elbow nozzle (3). The position of each component in the assembled device is observed in Figure 1d, where the infiltration chamber (Figure 1a) is screwed with the cover (Figure 1c) and placed in the spoon (Figure 1b).

Manufacture of a Pilot Device

According to the design presented in Figure 1a–d, real dimensions were selected for manufacturing a pilot device, which was used for manufacturing different metal foams by infiltration. These dimensions were selected due to the existence of commercial materials, easy to find, which fulfilled the necessities of the design. Figure 2a shows an isometric view of the pilot device with the dimensions

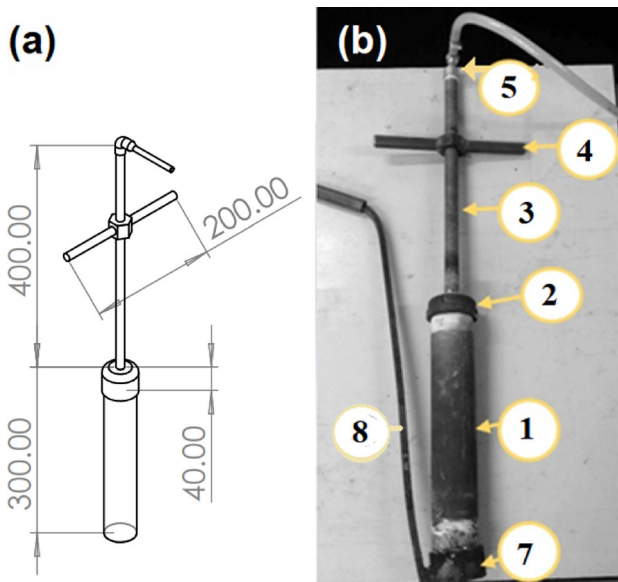


Figure 2. (a) Dimensions (in mm) of the device manufactured using the design proposed in Figure 1a-d, and (b) real manufactured device.

selected, drawn using SOLIDWORKS Premium 2022 SP2.0. The complete real pilot device manufactured using these dimensions is presented in Figure 2b. The infiltration chamber (1) is a 304L stainless steel cylindrical pipe, screwed in one of his ends, with an internal diameter of 5.08 cm, a wall thickness of 0.4 cm, and a height of 30 cm. This type of steel is one of the most common austenitic stainless steels, making it easy to find. It is cheaper than other steels with similar characteristics, it is not magnetic and has good machinability.³¹ Besides, the 304L stainless steel has important properties which makes it suitable for the application in this device, such as good corrosion resistance and wear behavior even up to 850 °C.³² It also has high strength at elevated temperatures, and a large number of industries take advantage of these properties, such as nuclear plants that use it in pipes for heat exchange, or for conducting fluids at high temperatures. 304L grade steel has lower C percentage than the conventional 304 steel (respectively have maximums of 0.03 and 0.07 %C), which is important for their anti-corrosion properties, affected for the higher presence of C in the conventional 304 steel.

The cover (2 in Figure 2b) of the device was made of galvanized steel, which can be also obtained commercially everywhere. The internal threading of this cover must match the external threading of the infiltration chamber (1 in Figure 2b). This cover was drilled at its center, where it was welded a tube (conduction tube 3 in Figure 2b) also made of galvanized steel. The length of this tube was 40 cm, with a diameter of 2.54 cm. Its purpose is for gas injection or fumes extraction. It is screwed at its superior end. The handling bar (4) is located at 30 cm from the base of the conduction tube. This bar consists of two solid 1045

steel bars of 2 cm in diameter, welded to a nut, which is also welded to the conduction tube. Threaded to the conduction tube it is the nozzle (5), consisting of a bronze elbow with 2.54 cm internal diameter and a copper tube (6), which is 7 cm long and 0.7 cm internal diameter. The connections are sealed with graphite adhesive tape to prevent leakage.

The spoon consisted of a cylindrical support (7 in Figure 2b), manufactured using a tube with internal diameter approximately equal to the external diameter of the infiltration chamber. This support is used for inserting the infiltration chamber in it, and as a controlling mechanism of the infiltration process, as it will be further observed. A square cross section bar (8) made of 1045 steel alloy was welded to the support for handling the device.

Device Operation

Once all the parts were manufactured, the device was ready for being used. Its operation consists on 6 steps: (1) preparation of preforms and alloys, (2) device assembly, (3) introduction of the device into a heating system (this is not part of the device), (4) alloy fusion and infiltration, (5) cooling, disassembly, and removal of the obtained material, and (6) removal of the space holders (only for conventional foams). These steps are presented below.

Preparation of Preforms and Alloys

For the infiltration process, specifically when a removable space holder phase (SHP) is included, preparing this phase as a preform is important for their correct removal in the final step. The preform can be composed by SHP or reinforcements, depending on the material to be manufactured. The preform can be used as separate particles or as a sintered preform. Characteristics of the preform such as chemical composition, size and packaging percentage affect the final structure and mechanical properties of the resulting material.⁵ Then, the preparation of the preform is an essential stage for manufacturing these materials. In the device here presented, previous to the inclusion of the preform, the infiltration chamber is inserted into the spoon, sealing the bottom of the chamber. This allows to add the preform by the open top of the tube, being the quantity of preform dependent on the desired final height of the material to be manufactured. After that, above the preform is placed the solid alloy, which can be inserted as small parts, or as a cylinder large enough to fill the hollow spaces of the preform. It is important to note that the use of a non-stick agent such as graphite or boron nitride is recommended in the inner parts of the infiltration chamber in contact with the preform and the alloy. This agent should be also spread on the spoon and the contact zones of the

parts of the device. This to avoid adhesions due to the high temperatures reached during the device operation.

Device Assembly

Once the SHP, reinforcement or preform and the alloy have been inserted into the infiltration chamber, the device is ready to be mounted. The cover is screwed to the infiltration chamber, while a gas injection line is connected to the nozzle part of the cover (see Figures 1a–d or 2a–b). It is desirable that a pressure gauge and regulator be installed immediately after the gas cylinder to control the gas injection (if necessary).

Heating System

Once the device is fully mounted it is necessary to insert it into a heating system. This is not part of the device, and can be any system that allows the device to be inserted into it, e.g., an electric oven. In Figure 3a, it is represented (using SOLIDWORKS Premium 2022 SP2.0) a heating system with the device inserted. It is desired to place the device inside a crucible on the bottom of the heating system (furnace). The crucible has the function of preventing any damage in the furnace if molten metal flows and escapes from the infiltration chamber/spoon joint. In our device we are using silica sand in this joint to avoid this phenomenon. The inclusion of the sand with small grains ($\sim 80 \mu\text{m}$) acts as a barrier, because their packing is considerably higher than for the NaCl grains. This leads to very small intergranular spaces between the sand grains, being necessary a higher pressure for infiltrating them. Besides, this facilitates the infiltration process without sealing the chamber bottom, and without loss of molten metal. In Figure 3b, we are including a real accommodation

of the device in a PREFINSA HR-C4 furnace, with external dimensions of 45 cm per side and an internal heating chamber of 22 x 22 cm of base and 28 cm in height. In order to avoid heat losses, an isolating material is surrounding the tube at the furnace entry. We are presenting this arrangement device-furnace as an example of the different possibilities of this device.

Alloy Fusion and Infiltration

After the introduction of the device into the heating system, the manufacturing process begins by increasing the temperature above the melting point of the alloy used for infiltration. Once this takes place infiltration can begin, fact which depends on the alloy system. This process could occur without gas injection if the fluidity of the used alloy is high enough to infiltrate the preform by gravity. If not, it is necessary the injection of gas (through the nozzle) to force the molten metal to infiltrate the empty spaces of the preform. The end of the infiltration process can be determined according to the characteristics of the alloy system, the size of the porosity to be infiltrated in the preform and the gas pressure; or can be visually determined when the molten metal starts to flow (droplets) from the bottom of the spoon.

Cooling, Disassembly, and Removal of the Material

Once the molten metal infiltrated the preform, the device is removed from the oven and placed on a bed of sand. The device is handled using simultaneously the bar and the spoon. A direct quenching could also be used if it is desired, introducing the device into a quenching medium. This procedure is not recommended in all cases since the crucible material is steel, which would shorten its useful life if the melting point of the used alloy for infiltration is higher than $\sim 720 \text{ }^\circ\text{C}$. For Al-alloys, this quenching is possible without affecting the device, because quenching temperatures are generally lower than $550 \text{ }^\circ\text{C}$. The advantage of rapid cooling is that in this way some defects can be avoided, like volumetric shrinkage, as Lara-Rodriguez et al.²² reported. The process will be the same in case of being needed gas pressure to infiltrate the preform, just adjusting the pressure necessary to make the molten metal flow, which mainly depends on the composition of the alloy (e.g., the addition of Si favors gravity infiltration due to its high fluidity). Once the infiltration chamber is cold, it is removed from the spoon and the cover is retired. Finally, the composite preform + alloy is pushed out from the infiltration chamber. The use of non-stick agents such as graphite or boron nitride (BN) in the inner of this chamber facilitates the ejection of the manufactured materials from the device. This was possible just by applying pressure on the top surface of the material.

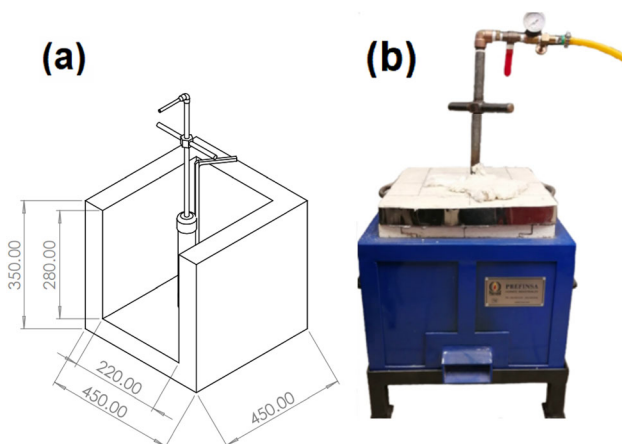


Figure 3. (a) Representation of the heating system used for the device operation (dimensions in mm), and (b) Real device introduced in a furnace, used for manufacturing metal foams.

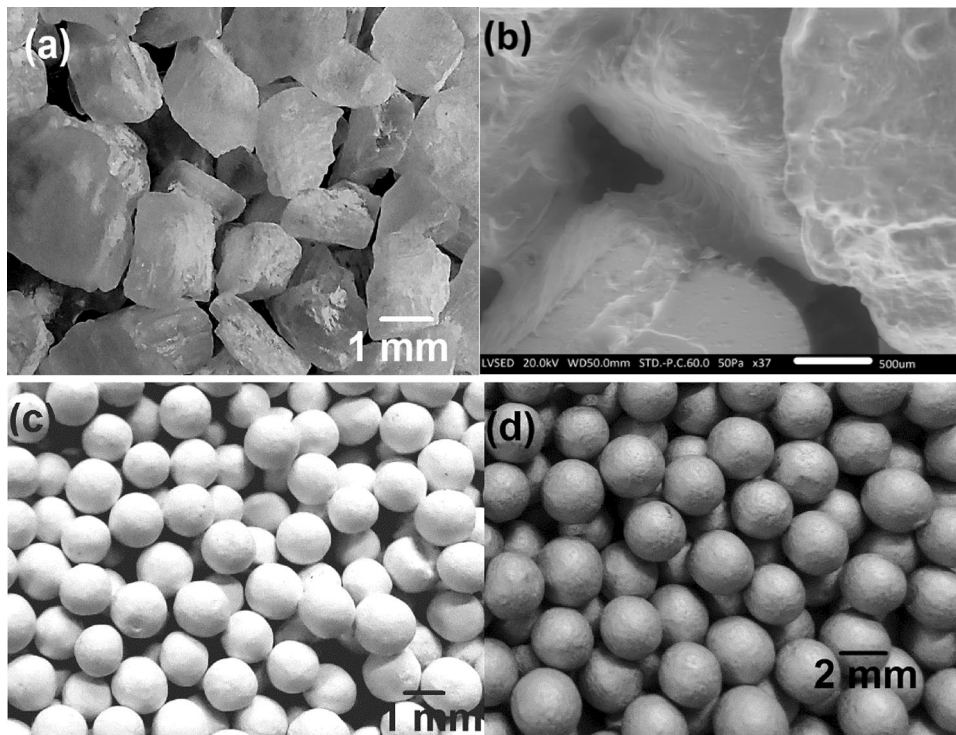


Figure 4. (a) OM of isolated NaCl particles used as space holders, (b) SE-SEM image of the SHP used as a preform after sintering NaCl at 780 °C during 1 h, (c) Al₂O₃ particles used for manufacturing the composite Al-Al₂O₃ foam, and (d) Fe hollow spheres for manufacturing syntactic foams.

Removal of the Space Holders

When the device is used for manufacturing conventional foams, the last step is the removal of the SHP. This in order to generate the characteristic porosity of the metal foams. Removal process depends on the selected material, and can be done using processes such as dissolution, solvent attack, vibration, or calcination.^{33,34} Once this process is completed, porosity is revealed, and the foam is ready to be characterized.

Study Cases as Examples of the Device Operation

Selection of the Materials

In order to show the effectiveness of the device, examples of the manufacturing process for different materials are presented in this section. Four aluminum alloys and one Cu-Sn alloy were used: a 332 (Al-10Si-3Cu in wt.%) alloy, three quaternary Al-7Mg-6Si-*x*Cu (*x* = 3, 5 and 7 wt.%) alloys, and a Cu20Sn alloy. Al-alloys were selected due to their high Si content, which increases fluidity. Cu content was modified in order to analyze if alloys with lower fluidity and different wettability can be also infiltrated using the device proposed in this work. The CuSn alloy was selected due to its higher melting point (~900 °C).

Depending on the material to be manufactured, several types of preforms can be used, including space holders, and solid or hollow spheres. The material of the preform must have a melting temperature higher than the melting point of the metal used, as has been reported by Ozer et al.³⁴ In this sense, NaCl particles are suitable for manufacturing Al-foams due to their higher melting point (801 °C) compared to the melting point of Al (660 °C). Then, the space holders used in this work for manufacturing conventional foams were sift NaCl particles of 2.3 ± 0.3 mm, which are shown in the optical micrograph of Figure 4a. In order to show the possibility of using these particles as a preform, a previous sintering process was used, as it is observed in the Scanning Electron Microscopy (SEM) image of Figure 4b, where necks between NaCl grains can be observed after sintering the particles at 780 °C during 1 h. This process was carried out inside the infiltration chamber of the device, showing that it can be also used for this purpose. On the other hand, composite foams were manufacturing mixing 50-50 NaCl and Al₂O₃ spheres of 2 mm, which can be observed in Figure 4c. Finally, iron hollow sphere preforms were used as reinforcement to infiltrate the CuSn alloy, and obtain syntactic foams. These iron spheres have a melting temperature higher than the CuSn alloy. These spheres were manufactured by (Hollomet GmbH, Germany), and have an average diameter of 3 ± 0.3 mm, with an average thickness of 130 ± 10 μm. Some of these spheres can be observed in Figure 4d.

Infiltration Process

Once the materials were selected, as a first step the preforms (NaCl, iron hollow spheres, or the mixture NaCl-Al₂O₃) were introduced into the chamber (previously coated with BN and inserted into the spoon). The height of the preforms were ~ 10 cm. Then, the aluminum or copper alloys were placed above the preforms, and the infiltration chamber was sealed with the cover. As was already mentioned, this device needs an external heating system, in this case the electric furnace of Figure 3b was used for this purpose. The characteristics of this type of furnace make it possible to work with the geometry of the device presented in this work, since they have the top open, and the infiltration chamber with the spoon is the only part inside the oven. The other components are far from heat, which make them easy to handle. Although in this work the furnace is an external source, another option could be the integration of the resistance system to the device, but this is not the case. Once the system was ready, the temperature was raised above the melting point of the alloys. Depending on the alloy, the use of an external gas pressure might be or not necessary to force infiltration through the preform. It was observed that the aluminum 332 alloy has enough fluidity to infiltrate by gravity (due to the high Si content) and no external gas pressure was needed, while the other alloys needed the use of gas to infiltrate the preforms (25–50 ft³h⁻¹ of argon pressure was used). Once infiltration was complete, the cooling stage begins removing the device from the oven, and placing it on a bed of sand for cooling. Once the device reached room temperature, the composites preform + alloy were extracted from the chamber. When the preform was NaCl, the material was placed in water for 3 hours to dissolve NaCl particles, which generated the final porosity to obtain the foam.

Characterization of the Experimental Materials

The study of the experimental materials obtained using the device proposed in this work consisted on optical and scanning electron microscopies (OM and SEM, respectively), porosity and density measurements, and compression test. OM were analyzed through macrographies, while SEM was carried out using a Jeol JSM IT300LV model operated at 20 kV, with secondary and backscattered electron images (SE and BSE, respectively). Porosity was measured using image analysis and relative density, which was calculated using direct weight and volume measurements of cylindrical samples. Density measurements were carried out using Archimedes method in an analytical balance Sartorius model QUINTIX 124-1S. Compression tests were performed using an Instron 1125-5500R testing machine with a crosshead speed of 0.5 mm/min, using cylinders of 19 mm in diameter and 15 mm in length, according to the ISO 13314:2011 Standard “Mechanical testing of metals–Ductility testing- Compression test for porous and cellular metals”, which specifies the conditions for testing porous and cellular metals with porosities higher than 50%.

Results and Discussion

Due to the functioning nature of this device, some key steps should be considered for its correct operation. Prior to the final adjustment of the device and its operation conditions, different samples were unsuccessfully manufactured, as it is observed in Figure 5a, b. The two most important defects were the lack and the excess of infiltration. In the first case, as it is observed in Figure 5a, the bottom of the cylindrical foam is incomplete, while solid Al is still on the

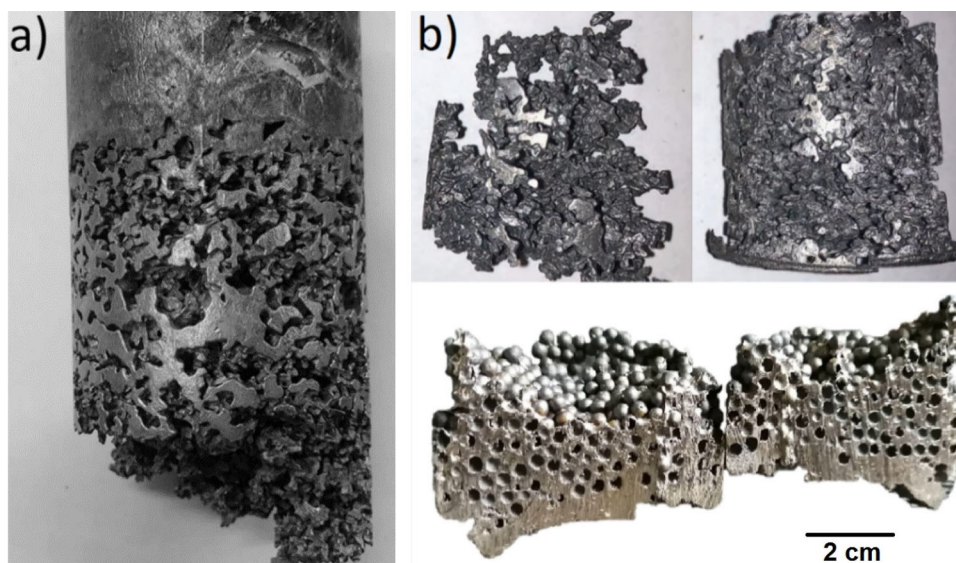


Figure 5. Incomplete foams, caused by inadequate control of the process parameters: (a) Lack of infiltration, and (b) Excess of infiltration.

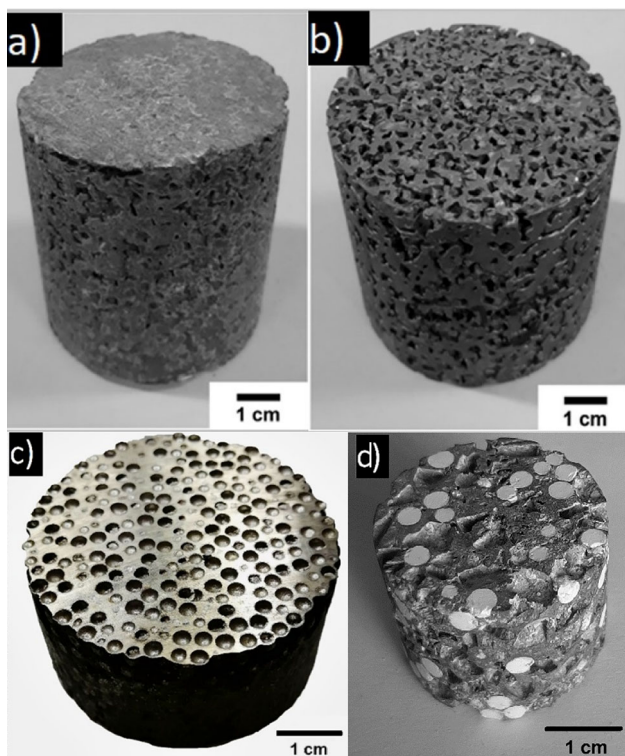


Figure 6. Macrographies of products obtained by infiltration with the device proposed in this work. (a) NaCl-Al composite, (b) Al conventional foam, (c) Copper matrix syntactic foam, and (d) Al matrix- Al_2O_3 composite foam.

top of the obtained material. The cause of this phenomenon could be the excessive sealed of the contact area between the infiltration chamber and the spoon, or the application of not enough gas pressure during the infiltration process. On the other hand, Figure 5b shows excessive infiltration, where the molten alloy poured out of the infiltration chamber, and the tops of the resulting materials were incomplete. This defect could be attributed to an excess of pressure or to problems in the sealed of the bottom of the infiltration chamber. This phenomenon was observed for the manufacturing process of both Al-alloy conventional foams (Figure 5b, top), and the Cu-Sn syntactic foam (Figure 5b, bottom).

After solving these manufacturing problems adjusting the process parameters, it was possible to obtain flawless materials, as it can be observed in Figure 6a–d. First, Figure 6a shows the composite formed by the Al-332 alloy and NaCl particles used as SHP, confirming that the entire infiltration process took place. Once NaCl was dissolved, a conventional Al-foam was obtained, as it is observed in Figure 6b. Figure 6c presents the syntactic foam obtained using the CuSn alloy, where the iron hollow spheres are uniformly distributed in the foam body. Finally, Figure 6d shows a composite foam Al- Al_2O_3 , where pores and reinforcements are observed, and the material was also obtained without defects. No excess or lack of infiltration or other defects are observed, demonstrating the

Table 1. Densities, Porosities and Relative Densities Obtained for the Foams Manufactured with Different Alloys and Space Holders

Obtained foam	Density (g cm^{-3})	Porosity (%)	Relative density
Foam AlCu3	0.93 ± 0.12	66 ± 2	0.34 ± 0.02
Foam AlCu5	0.88 ± 0.20	68 ± 5	0.32 ± 0.06
Foam AlCu7	0.91 ± 0.08	69 ± 3	0.31 ± 0.03
Composite foam Al 332- Al_2O_3	1.93 ± 0.29	38 ± 3	0.62 ± 0.08
Syntactic foam CuSn	4.42 ± 0.99	45 ± 5	0.53 ± 0.06

effectiveness of the device proposed in this work for manufacturing metal foams and composites with the different alloys used.

The range of porosities, reinforcement percentages and relative densities of the obtained materials is presented in Table 1. As can be seen, porosities for the conventional foams AlCu3, AlCu5 and AlCu7 were high, ranging from 66 to 69%. Differences in porosity could be a consequence of mixture conditions. The composite foams reinforced with NaCl presented a porosity of 38%, while the syntactic foams obtained using the CuSn alloy presented a porosity of 45%. For these materials, relative densities ranged from 0.31 to 0.62. These values have significant effect on the mechanical properties, as will be further analyzed. It is important to remark that measured densities of the used materials were: $\text{Al}_2\text{O}_3 = 3.4 \text{ g cm}^{-3}$, Al332 = 2.69 g cm^{-3} , AlCu3 = 2.74 g cm^{-3} , AlCu5 = 2.76 g cm^{-3} , AlCu7 = 2.95 g cm^{-3} , and Cu20Sn = 8.9 g cm^{-3} .

For a deeper analysis of the foams, longitudinal sections were cut to corroborate the interconnectivity of the pores, the correct infiltration of the molten Al-alloy, and the complete dissolution of the NaCl space holders. As it can be seen in the macrography of Figure 7a, no defects were observed. This fact can be corroborated in the SE-SEM image of Figure 7b, which shows the interconnection between pores. NaCl was not detected in the pores walls after dissolution, which agrees with other works where no reaction products were detected for Al-foams manufactured using NaCl as space holders, as showed the research by Carranza et al.²¹ and Reyes et al.³⁵. It is important to remark that different interactions may occur between the matrix alloys and the reinforcements or space holders, including modifications in the matrix microstructure and its precipitation process, diffusion of elements through the interfaces, change in the reinforcement wettability by the liquid metal, loss of alloying elements, and deterioration of the reinforcement.⁷ These reactions have been extensively studied, and depend among other parameters on the manufacturing process, temperature and time of infiltration,

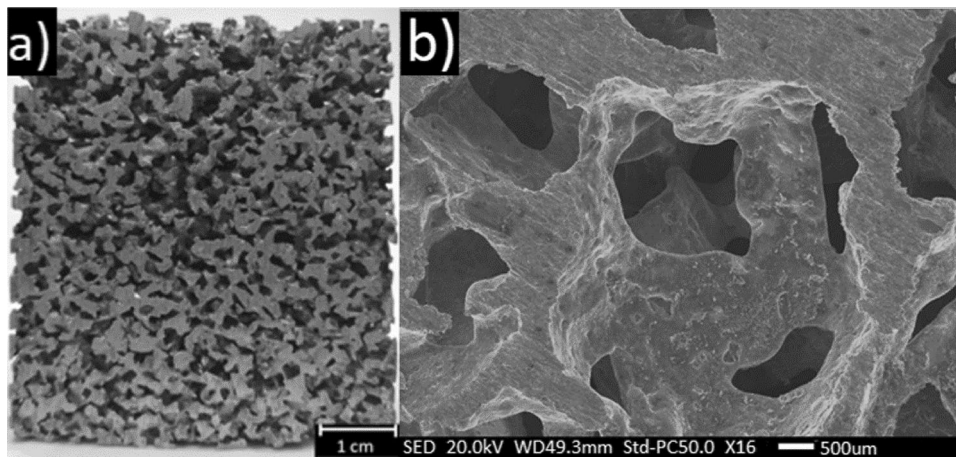


Figure 7. (a) Macrograph of the longitudinal section of an experimental Al matrix conventional foam, and (b) SE-SEM image of the foam where interconnection between the pores can be seen.

wetting of the system, and the chemical compositions of the matrix and the reinforcement. For the particular case of Al_2O_3 , reaction products are also limited because the system $\text{Al}-\text{Al}_2\text{O}_3$ does not react, although the presence of high content of some alloying elements (e.g. Mg) could contribute to interfacial reactions, as reported the work of Guerrero et al.⁷ In the composite foam reinforced with Al_2O_3 manufactured here, the absence of Mg for the alloy matrix $\text{Al}-10\text{Si}-3\text{Cu}$ did not contribute to generate interfacial reactions. Otherwise, for the interaction between solid Fe and molten Cu alloys some interfacial products such as CuFe_2O_4 have been reported, although the low surface energy of liquid Cu with respect to solid Fe limits the occurrence of interfacial reactions.³⁶ The study of these interactions was not among the objectives of this work, but it is our interest their research, which will be carried out modifying some manufacturing parameters, mainly increasing temperature and time of contact between the molten matrices and the reinforcements.

The microstructural analysis of the resulting materials shows the absence of microporosity in the matrices, as it can be observed in Figure 8a–d. In the case of Al-alloys, BSE-SEM images of Figure 8a–c show the characteristic phases of these alloys. First, Figure 8a shows the microstructure of the $\text{Al}-10\text{Si}-3\text{Cu}$ alloy, used for obtaining a composite foam infiltrating a mixture $50\text{NaCl}-50\text{Al}_2\text{O}_3$ (as the observed in Figure 6d). As it can be seen, Al_2Cu (light grey) and needle-like Al_5FeSi intermetallic (grey) are present, surrounded by the $\alpha\text{-Al}$ matrix. Si eutectic is also present in this alloy, barely observed due to the image mode. Otherwise, for the conventional foams obtained infiltrating NaCl preforms the microstructure is also free of defects. This is observed in Figure 8b, c for the alloys $\text{Al}-7\text{Mg}-6\text{Si}-3\text{Cu}$ and $\text{Al}-7\text{Mg}-6\text{Si}-5\text{Cu}$, respectively. In these cases, Q-phase ($\text{Al}_5\text{Mg}_8\text{Cu}_2\text{Si}_6$) and Mg_2Si are present together with Al_2Cu . Although these alloys present a lower content of Si and a higher content of other alloying

elements, they also infiltrated the preforms, without leading to any defect formation. Finally, Figure 8d shows a BSE-SEM micrograph of the CuSn matrix for the syntactic, showing a light phase ($\epsilon\text{-Cu}_3\text{Sn}$, 41%) and a darker one ($\alpha\text{-Cu}$, 59%). These results demonstrate that the device assured good infiltration, and can be used for different Al-alloys, but also for Cu-Sn alloys.

In order to probe the mechanical behavior of the obtained materials, Figure 9a and b shows the resulting stress-strain curves, with images inserted for different deformations for the cases of the composite $\text{Al332}-\text{Al}_2\text{O}_3$ foam and the syntactic $\text{Cu20Sn}-\text{Fe}$ hollow spheres foam. The experimental foams presented the characteristic stress-strain curve of the metal foams. According to literature, the parts of these curves are: (i) an initial linear elastic region at very low strain, (ii) an extended plateau region at a relative constant stress level, where the stress increases slowly as the cells deform and collapse, and (iii) a densification region where the collapsed cells are compacted together, increasing again the stress.³⁷ They presented different plateaus and densification regions, which depended on the porosity percentages, the use of reinforcements, and the microstructure of the solid matrix. The presence of different brittle second phases, with different morphologies, could be the cause of the different behaviors observed for the Al matrix foams with different Cu contents in Figure 9a.³⁸ The mechanical behavior for the composite foam reinforced with Al_2O_3 is significantly better, this because the significantly lower porosity percentage (only 38%, as was observed in Table 1), and because for this kind of materials the presence of the ceramic with high elastic modulus strengthens the matrix and hence the foam. That is why the plateau is more constant. Finally, the Cu-Sn syntactic foam (Figure 9b) presents the higher mechanical properties. First, due to the effect of the matrix, which has higher intrinsic mechanical strength than Al-alloys, and second due to the presence of the iron hollow spheres,

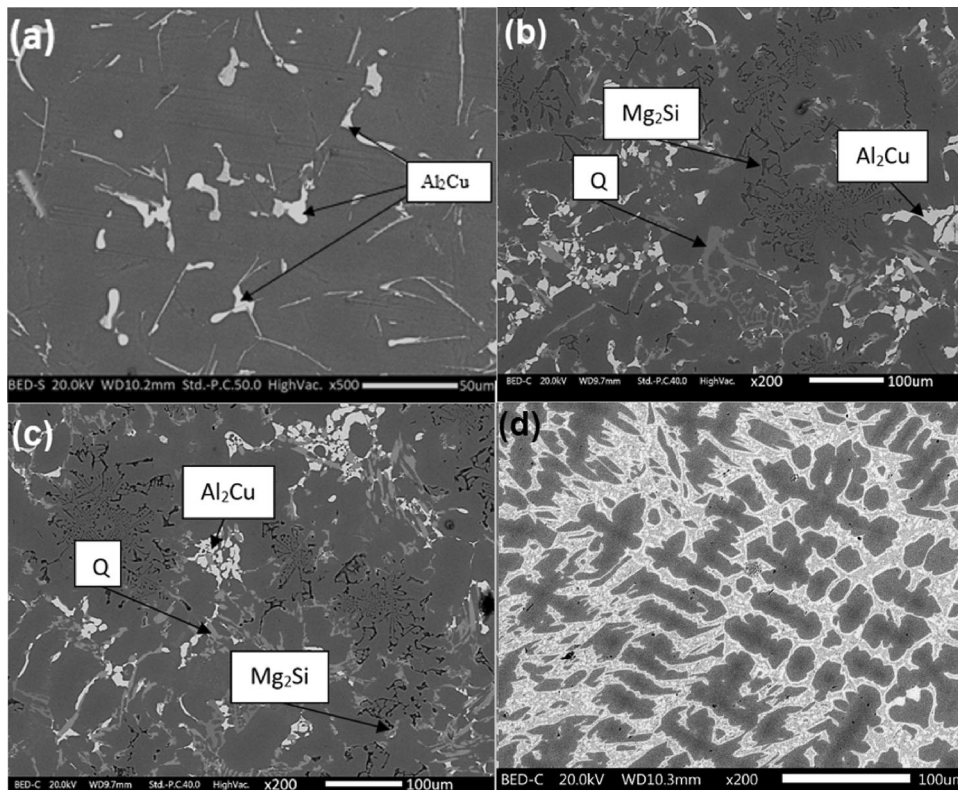


Figure 8. Microstructures for the alloy matrices for the manufactured foams: (a) 332 alloy, (b) AlCu3, (c) AlCu5, and (d) Cu-20Sn.

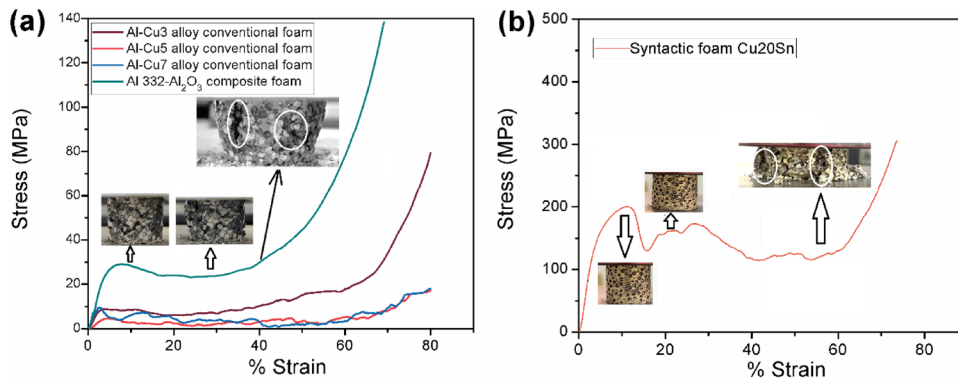


Figure 9. Stress-strain curves for: (a) Al matrix foams, and (b) CuSn syntactic foam.

which not only diminish density but also reinforces the material. In this case, the plateau is different due to the presence of these spheres, which collapse at different stages. Cell arrangement is another important characteristic affecting the mechanical properties of these foams, as reported by Binesh et al.⁵ for composite foams, leading to both brittle or ductile behaviors even for foams with similar relative densities. One or other behavior depends on parameters such as cell size, shape, and wall thickness, directly affected by the cell arrangement. The work of Verma et al.³⁹ also found the importance of these parameters for closed-cell conventional Al-foams obtained using TiH_2 as foaming agent. The images for deformations of

~ 10 % observed in Figure 9a and b, show the specimens mounted and with low deformation of the pores, while for 40 and 55% observed in Figure 9a, b, respectively, the deformations of the pores are already significant, with deformed cells and cracks (circled) which propagated along the specimen. These images captured during the deformation of the foams help to analyzed the brittle deformation mechanisms, consisting on the deformation and coarsening of the coarser cells, followed by cracking which leads to the foam failure. This behavior agrees with the reported by Verma et al.³⁹ in their research of the compressive response of closed-cell aluminum foams.

Table 2. Mechanical Parameters from the Stress–Strain Curves for the Manufactured Foams

Obtained foam	Young modulus (GPa)	Yield stresses (MPa)	Plateau average (MPa)	Stresses for densification (MPa)	Energy absorption (MJ m ⁻³)
Foam AlCu3	2.0 ± 0.2	8.2 ± 0.9	10.2 ± 0.3	16.3 ± 2.1	5.9 ± 1.0
Foam AlCu5	1.6 ± 0.2	3.1 ± 0.5	2.1 ± 0.1	4.2 ± 1.2	1.8 ± 0.2
Foam AlCu7	4.2 ± 0.6	8.5 ± 0.6	3.1 ± 0.3	6.6 ± 1.0	2.4 ± 0.6
Composite foam Al 332-Al ₂ O ₃	4.5 ± 0.5	28.7 ± 1.1	25.6 ± 1.6	29.8 ± 2.9	9.8 ± 0.9
Syntactic foam CuSn	47.2 ± 8.1	170.0 ± 10.1	140.5 ± 8.2	120.4 ± 8.8	79.7 ± 6.6

Table 2 shows the main parameters of the stress-strain curves for these foams, demonstrating the aforementioned related to the behavior of each foam. These results show that using the device it is possible to obtain different foams, with porosities and mechanical properties in correspondence with that reported in the literature,³⁷ depending on the space holder phase or reinforcement, and on the alloy used.

Conclusions

A device for foams and composite materials manufacturing by the infiltration method was designed and manufactured in the work presented. This device was successfully used with different Al-alloys and a CuSn alloy, infiltrating them through different reinforcements or space holders, such as NaCl particles, Fe hollow spheres, and a combination of NaCl and Al₂O₃ particles. Depending on some characteristics of the alloys and the space holder phase or reinforcement used, the device requires or not the use of an external gas pressure to infiltrate the molten alloy. For alloys with high Si contents and low quantity of other alloying elements the infiltration process occurs by gravity, advantage which made the process easier and cheaper. The device was also useful to produce foams with less fluid alloys, such as CuSn or Al-alloys with high content of Cu and Mg, applying Ar pressure to infiltrate the particles. In both cases, the manufacturing conditions were adjusted, being possible to obtain foams and composites without defects and with the characteristic mechanical properties of these materials. For conventional foams, porosity percentages ranged from 66 to 69%, with densities between 0.88 and 0.93 g cm⁻³, and relative densities from 0.31 to 0.34. Syntactic CuSn-Fe hollow sphere foams were also successfully obtained, with a porosity of 45%, while the composite Al 332-Al₂O₃ foam presented a porosity of 38%. All these materials presented the characteristic stress-strain curves for metal foams, and matrices without defects. In addition, this device is easy to operate, with a manufacturing cost significantly cheaper compared to other devices reported in literature. This makes it suitable for laboratory experiments and applications where small pieces with distinct characteristics are required.

Acknowledgments

The authors would like to acknowledge the financial support from SEP CONACYT 285215 and UNAM PAPIIT IN102322. O. Hernández and H. Mecinas Eliezer are also acknowledged respectively for their technical support in SEM and compression analyses.

Open Access This article is licensed under a Creative Commons Attribution 4.0 International License, which permits use, sharing, adaptation, distribution and reproduction in any medium or format, as long as you give appropriate credit to the original author(s) and the source, provide a link to the Creative Commons licence, and indicate if changes were made. The images or other third party material in this article are included in the article's Creative Commons licence, unless indicated otherwise in a credit line to the material. If material is not included in the article's Creative Commons licence and your intended use is not permitted by statutory regulation or exceeds the permitted use, you will need to obtain permission directly from the copyright holder. To view a copy of this licence, visit <http://creativecommons.org/licenses/by/4.0/>.

REFERENCES

1. F. Baumgartner, H. Gers, Industrialization of P/M foaming process, In *Metal Foams and Porous Metal Structures*, J. Banhart, M.F. Ashby, N.A. Fleck Eds., (1999) 73–79, Verlag MIT.
2. J. Banhart, Manufacture, characterisation and application of cellular metals and metal foams. *Prog. Mater. Sci.* **46**, 559–632 (2001). [https://doi.org/10.1016/S0079-6425\(00\)00002-5](https://doi.org/10.1016/S0079-6425(00)00002-5)
3. L.J. Gibson, M.F. Ashby, *Cellular solids: structure and properties*, (Cambridge University Press, 1997).
4. A. Rabiei, L.J. Vendra, A comparison of composite metal foam's properties and other comparable metal foams. *Mater. Lett.* **3**, 533–536 (2009). <https://doi.org/10.1016/j.matlet.2008.11.002>
5. F. Binesh, J. Zamani, M. Ghiasvand, Ordered structure composite metal foams produced by casting. *Inter. J. Metalcast.* **12**, 89–96 (2018). <https://doi.org/10.1007/s40962-017-0143-x>
6. Ç. Bolat, İ.C. Akgün, A. Gökşenli, Effect of aging heat treatment on compressive characteristics of bimodal aluminum syntactic foams produced by cold chamber

- die casting. *Inter. J. Metalcast.* **16**, 646–662 (2022). <https://doi.org/10.1007/s40962-021-00629-0>
7. C.T. Guerrero, F. González, T.E. Soto, C. Aguilar, I.A. Figueroa, G. González et al., An overview of the interactions between reinforcements and Al matrices with Si, Cu and Mg as alloying elements in aluminum matrix composites: case of oxide reinforcements. *Mater. Res.* **25**, e20210540 (2022). <https://doi.org/10.1590/1980-5373-MR-2021-0540>
 8. L. Pérez, R. Mercado, I. Alfonso, Young's modulus estimation for CNT reinforced metallic foams obtained using different space holder particles. *Compos. Struct.* **168**, 26–32 (2017). <https://doi.org/10.1016/j.compstruct.2017.02.017>
 9. G.A. Gegel, D.J. Weiss, Enabling technology for the design of short-fiber reinforced aluminum MMC components. *Inter. J. Metalcast.* **1**, 57–67 (2007). <https://doi.org/10.1007/BF03355418>
 10. N.M.S. Kumar, T.N. Shashank, N.U. Dheeraj et al., Coatings on reinforcements in aluminum metal matrix composites. *Inter. J. Metalcast.* (2022). <https://doi.org/10.1007/s40962-022-00831-8>
 11. A. Szlancsik, B. Katona, K. Májlínger, I.N. Orbulov, Compressive behavior and microstructural characteristics of iron hollow sphere filled aluminum matrix syntactic foams. *Materials* **8**, 7926–7937 (2015). <https://doi.org/10.3390/ma8115432>
 12. Ç. Bolat, İ.C. Akgün, A. Gökşenli, Effects of particle size, bimodality and heat treatment on mechanical properties of pumice reinforced aluminum syntactic foams produced by cold chamber die casting. *China Foundry* **18**, 529–540 (2021). <https://doi.org/10.1007/s41230-021-1133-4>
 13. A.D. Akinwekomi, J.A. Adebisi, A. Adediran, Compressive characteristics of aluminum-fly ash syntactic foams processed by microwave sintering. *Metall. Mater. Trans. A* **50**, 4257–4260 (2019). <https://doi.org/10.1007/s11661-019-05347-1>
 14. D. Károly, Z. Iklódi, A. Kemény, D.B. Kincses, I.N. Orbulov, Production and functional properties of graded Al-based syntactic metal foams. *Metals* **12**, 263 (2022). <https://doi.org/10.3390/met12020263>
 15. M.H. Ghaleh, N. Ehsani, H.R. Baharvandi, High-porosity closed-cell Aluminum foams produced by melting method without stabilizer particles. *Inter. J. Metalcast.* **15**, 899–905 (2021). <https://doi.org/10.1007/s40962-020-00528-w>
 16. J. Banhart, Metal foams: production and stability. *Adv. Eng. Mater.* **8**, 781–794 (2006). <https://doi.org/10.1002/adem.200600071>
 17. P. Ajay Kumar, P. Rohatgi, D. Weiss, 50 years of foundry-produced metal matrix composites and future opportunities. *Inter. J. Metalcast.* **14**, 291–317 (2020). <https://doi.org/10.1007/s40962-019-00375-4>
 18. S. Senthil, M. Raguraman, M.D. Thamarai, Manufacturing processes & recent applications of aluminium metal matrix composite materials: a review. *Mater. Today Proc.* **45**, 5934–5938 (2021). <https://doi.org/10.1016/j.matpr.2020.08.792>
 19. Ç. Bolat, İ.C. Akgün, A. Gökşenli, On the way to real applications aluminum matrix syntactic foams. *Eur. Mech. Sci.* **4**, 131–141 (2020). <https://doi.org/10.26701/ems.703619>
 20. L. Polonsky, S. Lipson, H. Markus, Lightweight cellular metal. *Mod. Cast.* **39**, 57–71 (1961)
 21. J.C. Carranza, L. Pérez, R. Ganesan, B.Y. Casas, R.A.L. Drew, C. Ruiz-Aguilar, I.A. Figueroa, I. Alfonso, Effect of fractal distribution of the porosity on mechanical properties of Al foams manufactured by infiltration. *J. Braz. Soc. Mech. Sci. Eng.* **41**, 379 (2019). <https://doi.org/10.1007/s40430-019-1876-7>
 22. G.A. Lara-Rodriguez, I.A. Figueroa, M.A. Suarez, O. Novelo-Peralta, I. Alfonso, R. Goodall, A replication-casting device for manufacturing open-cell Mg foams. *J. Mater. Process. Technol.* **243**, 16–22 (2017). <https://doi.org/10.1016/j.jmatprotec.2016.11.041>
 23. Y. Chino, D.C. Dunand, Creating aligned, elongated pores in Titanium foams by swaging of preforms with ductile space-holder. *Adv. Eng. Mater.* **11**, 52–55 (2008). <https://doi.org/10.1002/adem.200800232>
 24. J. Jakubowicz, G. Adamek, M. Dewidar, Titanium foam made with saccharose as a space holder. *J. Porous Mat.* **20**, 1137–1141 (2013). <https://doi.org/10.1007/s10934-013-9696-0>
 25. F. Mat Noor, M.I.M. Zain, K.R. Jamaludin, R. Hussin, Z. Kamdi, A. Ismail et al., Potassium bromide as space holder for titanium foam preparation. *Appl. Mech. Mater.* **465–466**, 922–926 (2014). <https://doi.org/10.4028/www.scientific.net/AMM.465-466.922>
 26. L. Stanev, M. Kolev, B. Drenchev, L. Drenchev, Open-cell metallic porous materials obtained through space holders-Part II: structure and properties. A review. *J. Manuf. Sci. Eng.* **139**, 050802 (2017). <https://doi.org/10.1115/1.4034440>
 27. Ç. Bolat, İ.C. Akgün, A. Gökşenli, Influences of reinforcement size and artificial aging on the compression features of hybrid ceramic filled aluminum syntactic foams. *Proc. Inst. Mech. Eng. C J. Mech. Eng. Sci.* **236**, 8027–8037 (2022). <https://doi.org/10.1177/09544062221083208>
 28. Ç. Bolat, B. Bilge, A. Gökşenli, An investigation on the effect of heat treatment on the compression behavior of aluminum matrix syntactic foam fabricated by sandwich infiltration casting. *Mater. Res.* **24**, e20200381 (2021). <https://doi.org/10.1590/1980-5373-MR-2020-0381>
 29. P. Pinto, N. Peixinho, F. Silva, D. Soares, Compressive properties and energy absorption of aluminum foams with modified cellular geometry. *J. Mater. Process. Technol.* **214**, 571–577 (2014). <https://doi.org/10.1016/j.jmatprotec.2013.11.011>
 30. M. González-Nava, A. Cruz-Ramírez, M.A. Suarez-Rosales, M.A.H. Pérez, Thermodynamic analysis of the aluminum alloy foaming process by melt route.

- J. Manuf. Process. **32**, 77–84 (2018). <https://doi.org/10.1016/j.jmapro.2018.01.028>
31. R.K. Desu, H. Nitin Krishnamurthy, A. Balu, A.K. Gupta, S.K. Singh, Mechanical properties of austenitic stainless steel 304L and 316L at elevated temperatures. *J. Mater. Res. Technol.* **5**, 13–20 (2016). <https://doi.org/10.1016/j.jmrt.2015.04.001>
 32. S. Karabeyoglu, E. Olcay, B. Ergene, C. Bolat, Wear performance of AISI 304L stainless steel under various ambient temperatures. *Lat. Am. Appl. Res.* **52**, 289–296 (2022). <https://doi.org/10.1016/j.jmrt.2015.04.001>
 33. M Bram, C Stiller, HP Buchkremer, Preparation and characterization of high-porosity titanium, stainless steel, and superalloy parts, In *Metal Foams and Porous Metal Structures*, J. Banhart, M.F. Ashby, N.A. Fleck Eds., (1999) 197–202, Verlag MIT.
 34. G. Ozer, K.A. Güler, Z. Taslicukur, Cellular aluminium foam metal production with space holder particles. *Mater. Test.* **52**, 379–382 (2010). <https://doi.org/10.3139/120.110140>
 35. C. Reyes, L. Béjar, J.C. Carranza, P. Pérez, L. Pérez, I. Alfonso, DEM-FEM combination for modelling and simulation of fractal metallic foams. *Mater. Today Commu.* **34**, 105054 (2023). <https://doi.org/10.1016/j.mtcomm.2022.105054>
 36. H. Huang, Z. Cheng, C. Lei, S. Tang, Y. Du, A novel synthetic strategy of Fe@Cu core-shell microsphere particles by integration of solid-state immiscible metal system and low wettability. *J. Alloys Compd.* **747**, 50–54 (2018). <https://doi.org/10.1016/j.jallcom.2018.03.013>
 37. R. Florek, F. Simancik, M. Nosko, J. Harnuskova, Compression test evaluation method for aluminium foam parts of different alloys and densities. *Powder Metall. Prog.* **10**, 207–212 (2010)
 38. K. Kim, A. Bobel, S. Baik, M. Walker, P.W. Voorhees, G.B. Olson, Enhanced Coarsening resistance of Q-phase in aluminum alloys by the addition of slow diffusing solutes. *Mater. Sci. Eng. A.* **735**, 318–323 (2018). <https://doi.org/10.1016/j.msea.2018.08.059>
 39. K.S. Verma, D. Muchhala, S.K. Panthi, D.P. Mondal, Influences of cell size, cell wall thickness and cell circularity on the compressive responses of closed-cell aluminum foam and its FEA analysis. *Inter. J. Metalcast.* **16**, 798–813 (2022). <https://doi.org/10.1007/s40962-021-00627-2>

Publisher's Note Springer Nature remains neutral with regard to jurisdictional claims in published maps and institutional affiliations.